Transportation Research Part D 158 (2026) 105397

Contents lists available at ScienceDirect

Transportation Research Part D

journal homepage: www.elsevier.com/locate/trd

# Evacuation dynamics and socioeconomic disparities during a tropical cyclone-blackout-heatwave compound hazard event

Xin Wang [a], Wei Zhai [b,*], Kerry Nice [a], Benteng Sun [c], Xueyin Bai [d], Haoming Qin [e], Huanchun Huang [e]

[a] Transport, Health and Urban Systems Research Lab, Faculty of Architecture, Building and Planning, The University of Melbourne, Melbourne, Australia
[b] Department of Public Affairs and Planning, University of Texas at Arlington, Arlington, TX, USA
[c] Department of Computer Science and Engineering, Hong Kong University of Science and Technology, Hong Kong SAR, China
[d] Program of Landscape Architecture, University of Texas at Arlington, Arlington, TX, USA
[e] School of Architecture and Planning, The University of Texas at San Antonio, San Antonio, TX, USA

ARTICLE INFO

*Keywords:*
Compound disaster
Hurricane evacuation
Heatwave
Human mobility

ABSTRACT

The increasing frequency of compound disasters, like 2024's Hurricane Beryl (tropical cyclone, blackouts, and extreme heat) in Texas, challenges traditional evacuation models, as the dynamics of cascading threats are poorly understood. Using aggregated, high-resolution location data and a multi-stage analytical framework, we show that cascading blackouts under extreme heat triggered a delayed but significant increase in evacuation, with outage-affected communities exhibiting daily evacuation rates 3.0 percentage points higher after landfall than comparable non-outage communities. Spatial lag analysis further indicates that evacuation responses were clustered across neighboring communities. Furthermore, Explainable Machine Learning (XGBoost-SHAP) reveals that socioeconomic factors and racial composition were stronger predictors of evacuation than outage and heat exposure. Crucially, the proportion of white residents was the most powerful positive predictor of leaving. These findings suggest that compound disasters can simultaneously stimulate evacuation while exposing deep inequalities in who is able to respond effectively, underscoring the need for equity-centered disaster planning.

## 1. Introduction

Climate change is intensifying both the frequency and severity of natural disasters. A rapidly growing threat is the phenomenon of compound events in which multiple hazards occur concurrently (IPCC, 2021; Gori et al., 2022; Marsooli et al., 2019; Xi et al., 2023), such as droughts coupled with heatwaves (Perkins-Kirkpatrick and Lewis, 2020; Zscheischler et al., 2018), floods coupled with landslides (Liao et al., 2021; Zscheischler et al., 2020), and wildfires coinciding with hazardous air pollution (Jaffe et al., 2020; Gould et al., 2024). Compound disasters present a uniquely dangerous scenario, directly threatening public health and complicating evacuation decision-making, amplified by multiple interconnected factors. For instance, in the southern United States, TCs season runs from June to November and often directly overlaps with the peak of summer heat, creating simultaneous exposure to storm impacts and high temperatures (National Hurricane Center, 2026). In addition, TCs are a primary cause of extended blackouts (Marsooli

* Corresponding author.
*E-mail addresses:* xin.wang.10@student.unimelb.edu.au (X. Wang), wei.zhai@uta.edu (W. Zhai), kerry.nice@unimelb.edu.au (K. Nice), smark2019@outlook.com (B. Sun), xueyin.bai@uta.edu (X. Bai), haoming.qin@utsa.edu (H. Qin), huangyanlin2010@163.com (H. Huang).

https://doi.org/10.1016/j.trd.2026.105397
Received 16 November 2025; Received in revised form 21 April 2026; Accepted 22 April 2026

et al., 2019), disabling the air conditioning systems crucial for surviving extreme heat. Thus, while sheltering in place may be feasible during cyclones, adding compounding blackouts and heatwaves eliminates shelter in place as a suitable option requiring more complex evacuation imperatives (Wu et al., 2022). However, prior compound hazard research has primarily emphasized infrastructure resilience modeling (Feng et al., 2022) or theoretical risk assessments (Matthews et al., 2019), while lacking empirical behavioral evidence on evacuation decision-making under these compound conflicting pressures.

On the other hand, evacuation research has largely focused on single hazards or relied on post-event surveys and stated intentions (Huang et al., 2016; Feng and Lin, 2022; Yabe and Ukkusuri, 2020; Deng et al., 2021), which are vulnerable to recall bias and provide limited real-time behavioral evidence. This study fills these gaps by leveraging aggregated, high-resolution mobility data to investigate evacuation dynamics during Hurricane Beryl (2024) in Texas, a compound disaster characterized by TC, rolling blackouts, and extreme heat. We test the following three key hypotheses:

**H1:** The compound hazards of power outages and extreme heat will trigger a significant wave of delayed evacuations. We hypothesize that untenable living conditions created by the loss of air conditioning during a heatwave will compel households, who initially decided to shelter in place, to evacuate after the hurricane has passed. This hypothesis is tested using a difference-in-differences (DID) model to isolate the causal impact of power outages on daily evacuation rates.

**H2:** Socially vulnerable communities will have a weaker capacity to evacuate after the onset of power outages. We hypothesize that lower-income communities, racial minority communities, and communities with limited mobility resources will face greater systemic barriers to evacuation under compound disaster conditions. To assess these disparities, we first use Spatial Lag Regression (SLR) to establish baseline spatial correlations while explicitly accounting for spatial dependence in evacuation rates, and then apply XGBoost-SHAP to identify non-linear and heterogeneous vulnerability patterns.

**H3:** Evacuation decisions will exhibit positive spatial dependence. We hypothesize that a community's evacuation rate is significantly influenced by the evacuation rates of its neighboring communities, indicating spatial spillover effects in decision-making. This hypothesis is tested within the SLR by quantifying the significance of the spatial lag term.

## 2. Literature review

### 2.1. Tropical cyclones-Blackout-Heatwave compound disaster

Compound disasters, where multiple interdependent events produce a greater impact than the sum of their parts, are a primary driver of weather- and climate-related catastrophes (Zscheischler et al., 2018, 2020). Among these, the co-occurrence of TCs, widespread blackout, and extreme heatwave represents a compound disaster of growing concern. TCs are powerful meteorological events that serve as triggers for cascading disasters. Specifically, TCs can compound with extreme heat to elevate post-landfall risk and exposure (Matthews et al., 2019; Wu et al., 2022), and generate multi-pathway coastal hazards through rainfall, storm surge, and flooding (Liao et al., 2021; Gori et al., 2022). Besides, the failure of the grid during TCs leads to widespread blackouts (Alemazkoor et al., 2020; Feng et al., 2022). In the United States, TCs are the leading cause of outages affecting over 100,000 customers for more than 24 consecutive hours (U.S. Department of Energy, 2021). The risks are amplified when blackouts coincide with heatwaves. Extreme heat is a major public health threat, especially for the elderly and socially disadvantaged with limited housing, mobility, and adaptive capacity (Ebi et al., 2021; Lee, 1980).

The unique danger of the TC-Blackout-Heatwave event stems from cascading failures of infrastructure and public health systems. By eliminating access to cooling, a concurrent heatwave transforms homes into heat traps and creates complex evacuation dilemmas. Climate change is projected to dramatically increase the frequency and severity of such events (Marsooli et al., 2019; Gori et al., 2022; IPCC, 2021). While storm surges were once the main hurricane-related fatalities (Lin et al., 2012), recent studies emphasize the combined threat of TCs and heatwaves. A 40-year study in Vietnam found that compound events involving heatwaves, heavy rainfall, and TCs are rising with increasing temperatures (Tung et al., 2024). Similar patterns are evident in the U.S., with projections showing that under high-emission scenarios, such compound disasters could become 17 times more frequent by 2100, increasing from once every 278 years to once every 16.2 years (Lin et al., 2024; Marsooli et al., 2019). This trend poses escalating threats to urban infrastructure and human health, particularly in regions facing prolonged heat during outages.

In synthesis, the compound-disaster literature has made substantial progress in quantifying hazard co-occurrence, grid vulnerability, and infrastructure disruption, yet it remains dominated by physical and engineering perspectives. What is still largely missing is real-time empirical evidence on how people behaviorally respond when these hazards unfold together rather than in isolation. This gap is especially consequential because evacuation under compounding risk is not determined by exposure alone, but by the interaction between infrastructure failure, thermal stress, and social capacity.

### 2.2. Differences in disaster perceptions of hurricanes and heatwaves

The adaption and evacuation process is strongly shaped by perception, alongside physical and socioeconomic conditions. Previous studies identify three groups of factors: cognitive (e.g., risk perception, outcome efficacy), affective (e.g., fear or worry), and social-contextual (e.g., descriptive norms and evacuation orders) (van Valkengoed and Steg, 2019). Among these, outcome efficacy and negative affect are most strongly correlated with evacuation. These perception-based elements can be considered under the broader category of disaster perception. For example, as a hurricane approaches, residents integrate forecasts and evacuation orders with household-specific conditions such as location, traffic, age, family composition, previous experience, property status, time of day,

and personal interpretation of the prediction and orders (Huang et al., 2016; Yabe and Ukkusuri, 2020), to decide whether, when, where, and how to evacuate (Feng and Lin, 2022).

While hurricane risks perception is generally high, perception of heatwave risk has been relatively underestimated (Howe et al., 2019), often leading to underestimation of secondary hazards such as heat exposure during TC–blackout–heatwave disasters. In Hurricane Beryl, this perception gap meant that some residents who initially chose to shelter in place anticipated the storm impacts but underestimated how quickly prolonged outages would eliminate air conditioning and turn indoor environments into dangerous heat exposure, delaying protective action. This disparity stems from hurricanes' visible destruction and extensive media coverage. Although research on heat hazards has expanded, heatwaves remain underrepresented in public discourse and disaster frameworks (van Valkengoed and Steg, 2019). Yet heatwaves are intensifying in frequency, and duration, with projections showing further increases under global warming (Perkins-Kirkpatrick and Lewis, 2020). Extreme heat is far deadlier than many natural hazards, killing on average more than twice as many people annually as hurricanes and tornadoes (U.S. National Weather Service, 2024). However, heat is not included in the list of disasters eligible for assistance from the Federal Emergency Management Agency (FEMA), as it is absent from the Stafford Act—the federal law that grants FEMA authority to respond to emergencies (CNN, 2023).

Taken together, this literature suggests a systematic asymmetry in how humans perceive hurricanes and heatwaves: hurricane risk is salient, visible, and institutionally amplified, whereas heat risk is often normalized, underestimated, or treated as secondary. Yet most existing evidence comes from surveys, reported intentions, or retrospective accounts, which cannot precisely capture whether this perceptual asymmetry translates into delayed protective behavior during a rapidly evolving compound event. This creates a second gap: the need for temporally resolved behavioral validation.

### 2.3. The inequality in responding to disasters

Spatial injustice and the heightened vulnerability of disadvantaged groups during evacuations are evident in compound disasters, particularly in TC-Blackout-Heatwave Compound Disasters. First, regarding infrastructure, studies indicate that low-income communities suffer significantly longer power outages, as seen in the delayed recovery times following Hurricane Isaac—vulnerable populations often experience longer power outages (Best et al., 2022; Karakoc et al., 2020; Rodriguez et al., 2022). Second, regarding mobility, wealth and racial composition act as strong predictors of evacuation, with minority households facing greater obstacles to leaving (Deng et al., 2021; Gu et al., 2024). Third, regarding infrastructure, resource-poor neighborhoods with limited social capital recover more slowly (Coleman et al., 2023; Hong et al., 2021).

However, significant gaps remain in understanding how these inequalities intersect during cascading TC-blackout-heatwave events. Prior studies have explored inequalities in individual hazards such as hurricanes or heatwaves (Adeola and Picou, 2016; Bolin and Kurtz, 2017; Laska and Morrow, 2006; Yabe and Ukkusuri, 2020), but few analyses investigate their intersection in cascading events. Furthermore, existing studies often rely on retrospective surveys (Houston et al., 2014; Reinhardt, 2015), which are prone to recall bias and fail to capture real-time behavioral nuances. Addressing this gap is critical for developing equitable preparedness and response strategies, especially as the frequency and intensity of compound disasters increase with climate change.

### 2.4. Research gaps

Despite growing recognition of the risks posed by TC-Blackout-Heatwave compound disasters, significant gaps persist in the literature. First, existing research emphasizes meteorology and power recovery, with limited attention to the behavioral and social dimensions of human response. Specifically, few large-scale quantitative studies examine how socioeconomic differences shape perceptions, evacuation, and coping strategies under these complex scenarios. This gap is critical because community responses can strongly influence overall risk, independent of hazard frequency or intensity. Second, while single-hazard evacuation is well-documented, the evacuation decision-making dynamics under the cascading pressures of compound TC-Blackout-Heatwave disasters remain poorly understood. Finally, methodological limitations hinder understanding, as traditional reliance on retrospective surveys is subject to recall bias and often fails to capture the precise timing of events, underscoring the need for large-scale, real-time behavioral data.

This study addresses these gaps by integrating behavioral, environmental, and infrastructural perspectives. Using large-scale mobility data from the 2024 Hurricane Beryl event within a multi-stage analytical framework, we employ DID to identify which hazard component most strongly triggers evacuation, use SLR to analyze changes in evacuation patterns before and after heat exposure due to outages, and XGBoost-SHAP to quantify socioeconomic and racial disparities in outcomes. By moving beyond static survey snapshots to dynamic behavioral analysis, the research contributes to a more comprehensive, human-centered framework for climate adaption and disaster resilience.

## 3. Data and methods

To answer these questions, we use smart device geolocation records collected during the 2024 Hurricane Beryl in Texas, combined with satellite observations indicating power outages and ambient temperature. Methodologically, we first apply spatial lag regression (SLR) to establish baseline correlations and spatial patterns, then use a difference-in-differences (DID) design to identify the causal effects of compound disasters. Finally, XGBoost models capture heterogeneity across groups, and SHAP analysis clarifies why certain populations face greater constraints and delayed evacuation (Fig. 1).

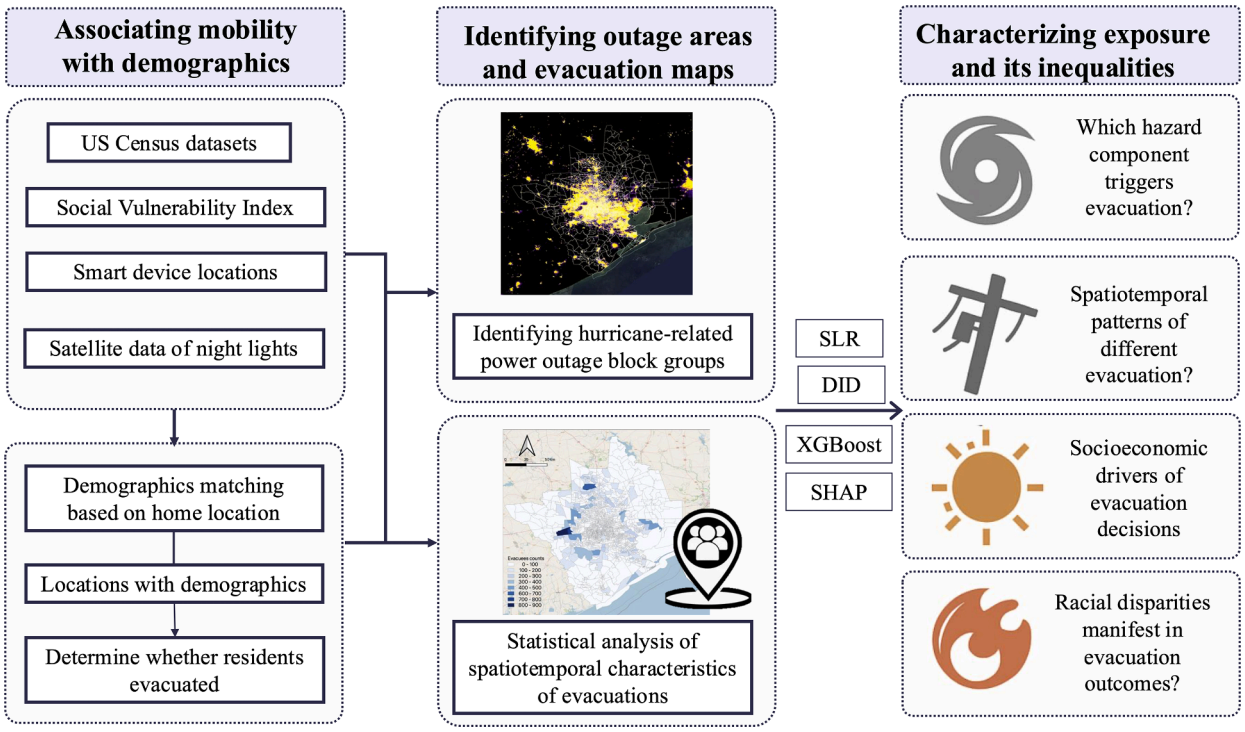


**Fig. 1.** The framework of this study. The framework integrates multiple datasets (U.S. Census socioeconomic indicators, mobile device locations, and VIIRS nighttime lights) to link mobility with demographic attributes. Power outage block groups related to Hurricane Beryl are identified from satellite data, and evacuation behaviors are derived by matching residents' home locations at the census block group level. These data are analyzed in three complementary steps: SLR to capture global correlations and spatial patterns, DID to estimate the causal impact on evacuation, and XGBoost with SHAP to reveal heterogeneous socioeconomic drivers and inequalities in evacuation outcomes.

### *3.1. Case study: the 2024 hurricane beryl event in texas*

Hurricane Beryl made landfall in Houston, TX on July 8, 2024, as a Category 1 storm. Though it weakened rapidly inland, its cascading effects on infrastructure were severe. The hurricane caused widespread outages, leaving over 220,000 homes and businesses without power, with Houston particularly hard-hit. Recovery was hampered by downed trees and damaged infrastructure, with costs exceeding $1 billion (Reuters, 2024). Prolonged outages coincided with extreme heat and humidity, creating a major public health crisis. By September 2024, heat-related death in the Houston area had reached to 40, underscoring the lethality of this compound hazard (Houston Public Media, 2024).

This study defines two primary analysis periods. The pre-outage phase (July 1–7) captures evacuation and preparedness travel before landfall, when the hurricane threat prompted warnings and pre-emptive evacuations. The post-outage phase (July 8–14) reflects the compounded hazards of extreme heat and continuing outages. The main threat during the pre-outage was the approaching hurricane, which prompted official warnings and pre-emptive evacuations. In contrast, the post-outage phase after landfall was dominated by compounded hazards of extreme heat exposure and the ongoing power outages. To avoid distortion from weekend travel, only weekday data are used for both phases.

### *3.2. Location data and preprocessing*

We used anonymized, aggregated location data to analyze human behavior following Hurricane Beryl. It provides visit data at the points-of-interest level. To ensure privacy, these datasets do not include home and workplace addresses and instead resolve to census block groups, and all mobility data analysis is conducted at the census block group level and presented in aggregated form. Sensitive locations, such as places related to healthcare, school, places of worship, or military service, are excluded from these datasets. This research focuses on the Houston Metropolitan Statistical Area (MSA) in Texas. As the most populous city in Texas and one of the largest metropolitan areas in the United States, the Houston MSA is home to over seven million residents. Its Gulf Coast location makes it highly vulnerable to TCs. To identify evacuees from the location data and their origin-destination (OD) pairs, we follow prior studies that use spatiotemporal constraints of user activities as the primary criterion (Washington et al., 2024; Liu et al., 2025). Consistent with existing definitions, where threshold ranges from one day (Anyidoho et al., 2023; Long et al., 2020; Younes et al., 2021) to three days (Cheng, 2021), we define evacuees as individuals not returning to their home location for at least 24 hours starting from 6 PM on the day of evacuation.

Because mobility-based evacuee identification is potentially sensitive to the choice of absence threshold, we validated the 24-hour rule along two complementary dimensions, with full results reported in Appendix A. First, we re-derived daily evacuation rates under 12-hour and 48-hour alternative thresholds and compared the resulting locations for outage and non-outage communities (Figure A1). Although the absolute evacuation rates differ across thresholds (as expected, since longer thresholds mechanically exclude shorter trips) the temporal dynamics of the outage gap are highly stable: the daily difference between outage and non-outage communities is correlated at $r = 0.991$ between the 12-hour and 24-hour definitions and at $r = 0.785$ between the 24-hour and 48-hour definitions, and all three thresholds locate the post-landfall surge on July 11–12. Inspection of the underlying trips confirms that the 12-hour threshold inadvertently captures routine commuting and non-evacuation overnight trips, introducing substantial noise, while the 48-hour threshold excludes short-term evacuees who sought temporary shelter nearby and returned within a day. The 24-hour threshold therefore provides the most robust balance between filtering routine travel and capturing diverse evacuation behaviors, while preserving the temporal pattern that drives our subsequent analyses.

Second, to verify that the observed contrast between outage and non-outage communities is not an artifact of the spatial structure of the device sample, we conducted a permutation-based placebo test in which the binary outage label was randomly reassigned across block groups 1000 times (Figure A2). The observed July 11, outage effect (0.0324) lies far outside the resulting 99% placebo interval of $[-0.0157, 0.0138]$, with an empirical $p$-value below 0.001, indicating that the measured gap cannot plausibly be reproduced by arbitrary spatial assignment of the treatment label. Together, these two checks support the robustness of our evacuee identification procedure; full details are reported in Appendix A.

### 3.3. Satellite data processing

To identify areas affected by power outages during the disaster, we utilized VIIRS nighttime light (NTL) data with a spatial resolution of 15 arc-seconds (approximately 500 m), obtained from satellite observations (National Centers for Environmental Information, 2024). NTL data, which capture artificial lighting, are an effective indicator of urban activity and infrastructure stability (Shi et al., 2016). Due to cloud cover from the hurricane, multi-day composites were not feasible, so we selected the best single image for each phase using the VIIRS Cloud Mask product. For the pre-disaster baseline, we used the image from July 4, 2024, the most cloud-free observation in the week before landfall. For the post-disaster period, we used July 9, 2024, the first clear image after the storm. This snapshot proxies post-landfall outages because widespread power loss began on July 8, and persisted for days, with over 1.6 million customers still without electricity on July 10, and substantial outages continuing thereafter (Dance, 2024; Jordan and Cobler, 2024; NOAA, 2024).

We employed a before-after comparison of NTL intensity before and after the storm to identify significant reductions in light emissions. A 15-unit reduction threshold was set to distinguish true power outages from temporary declines unrelated to infrastructure failure. This study-specific threshold was determined through sensitivity analysis to optimize detection of known outage areas. Specifically, we tested thresholds ranging from 10 to 30 units (including 10, 12, 15, 18, 20, 25, and 30). Relative to the 15-unit baseline (972 block groups classified as outage; 32.02% of all 3036 block groups), the outage classification changed modestly for nearby thresholds, indicating that outage delineation is relatively stable around the selected threshold. The methodology follows foundational literature on the NASA's Black Marble product suite (Roman et al., 2018, 2019), which establishes principles for distinguishing anomalies from background noise. This approach enabled precise identification of power outage communities (Fig. 2), critical for understanding spatial variations in disaster impact and evacuation.

### 3.4. Socio-demographic data

Community-level socioeconomic and demographic data were compiled from two public sources. Most variables, including income, unemployment, vehicle ownership, age, and racial composition, were obtained from the 2015–2019 American Community Survey (ACS) 5-year estimates at the Block Group level (U.S. Census Bureau, 2022). Two key vulnerability indicators, disability status and the percentage of single-parent households, were sourced from the Centers for Disease Control and Prevention's (CDC) 2018 Social Vulnerability Index (SVI) (Flanagan et al., 2011), derived from the 2014–2018 ACS 5-year estimates and provided at the Census Tract level. Block Groups are the smallest unit for which detailed sample data from ACS is released, typically containing 600–3,000 residents, while Census Tracts are larger units that generally contain 1,200–8,000 residents (U.S. Census Bureau, 2022). For consistency, the SVI indicators provided at the Census Tract level were spatially assigned to their constituent Block Groups, ensuring all variables were aligned at the uniform Block Group scale. A detailed description of all variables is provided in Table 1, which also presents descriptive statistics for the Houston MSA. These statistics are aggregated at the Block Group level, with a total of 3036 observations.

### 3.5. Extreme heat data and compounding conditions

To establish the heatwave component of the compound disaster, we compiled daily meteorological data for the study period. Historical weather records for the Houston, including maximum and minimum temperatures and humidity, were obtained from NOAA's National Centers for Environmental Information (NCEI) database (National Centers for Environmental Information, 2024b). This allows for a temporal analysis of the environmental stressors faced by the population.

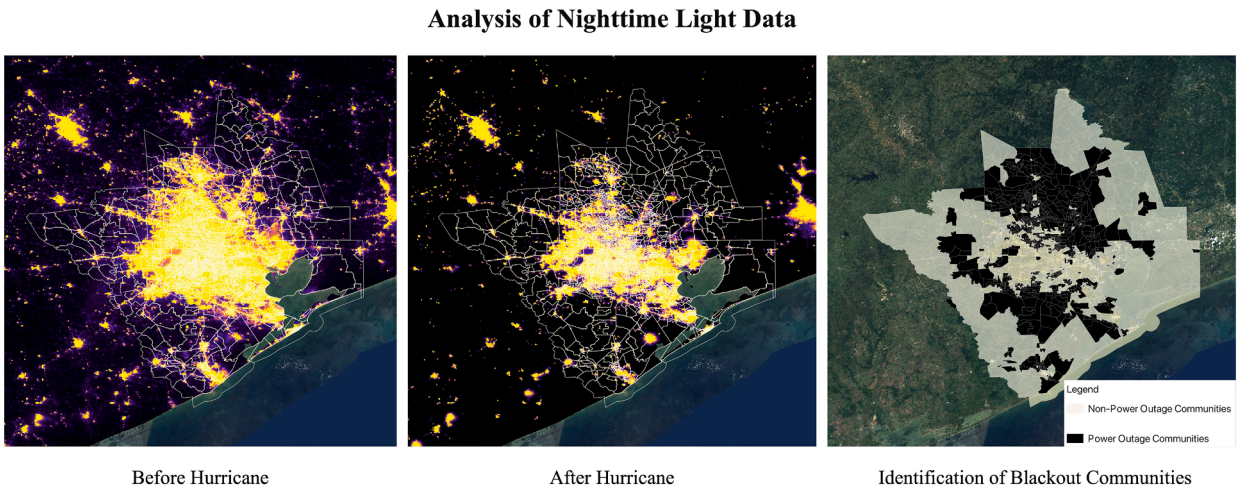


**Fig. 2.** Nighttime Light Changes and Blackout Communities. The left panel shows pre-disaster NTL brightness on July 4, 2024, and the middle panel shows the post-disaster NTL on July 9, and the right panel maps block groups with significant light reductions (interpreted as power outages).

**Table 1**
Descriptive Statistics of Community-Level Socio-demographic Variables.

| Variable | Mean | Std. Dev. | Minimum | Maximum |
|---|---|---|---|---|
| **Socioeconomic Status** | | | | |
| Median Household Income | 72,330.10 | 43,360.40 | 10,467.00 | 250,001.00 |
| Unemployment Rate (%) | 0.062 | 0.035 | 0 | 0.428 |
| Poverty Rate (%) | 0.145 | 0.123 | 0 | 0.826 |
| **Household Characteristics** | | | | |
| Number of Households | 795.8 | 782.9 | 74 | 16,932.00 |
| Single-Parent Households (%) | 0.378 | 0.277 | 0 | 0.833 |
| **Demographics** | | | | |
| Population Density (per sq. km)[1] | 2,113.40 | 2,305.30 | 1.2 | 27,710.70 |
| Population over 65 (%) | 0.116 | 0.053 | 0.005 | 0.435 |
| Population under 17 (%) | 0.256 | 0.064 | 0.013 | 0.419 |
| Male to Female Ratio | 1.002 | 0.155 | 0.505 | 2.427 |
| **Race & Ethnicity** | | | | |
| White Population (%) | 0.37 | 0.287 | 0 | 1 |
| Black Population (%) | 0.163 | 0.206 | 0 | 1 |
| Hispanic Population (%) | 0.389 | 0.273 | 0 | 1 |
| Asian Population (%) | 0.058 | 0.096 | 0 | 0.762 |
| **Vulnerability & Mobility** | | | | |
| Population with a Disability (%) | 0.104 | 0.046 | 0.011 | 0.392 |
| Households with No Vehicle (%) | 0.061 | 0.06 | 0 | 0.529 |
| Vehicles per Household | 1.801 | 0.32 | 0.555 | 2.625 |

[1] Unit for population density is assumed to be persons per square kilometer.

As shown in Table 2, July 1, to 14 was characterized by an oppressive and sustained heatwave. The heat index, which measures perceived temperature by accounting for humidity (Steadman, 1984), consistently exceeded 100°F (37.8 °C) and reached a dangerous high of 110°F (43.3 °C). Crucially, this heat stress was not limited to daytime. Minimum nighttime temperatures frequently remained near 80°F (26.7 °C), preventing the cooling needed for physiological relief. Prior research shows that elevated nighttime temperatures significantly increase heat-related morbidity and mortality by limiting the body's recovery (Loughnan et al., 2010; Nicholls et al., 2008).

This persistent, life-threatening heat is a critical piece of the story. While the hurricane's landfall caused an acute impact, the heatwave—a sustained stressor—amplified public health risks during widespread power outages. For households without electricity, the lack of air conditioning turned homes into heat traps. Because these extreme heat conditions were largely uniform across the Houston metropolitan area, the study can isolate how communities responded to power outages given their socio-demographic characteristics. The disaster thus reflects compounding of forces: pre-storm warnings, the physical impact of the landfall, widespread power outages, and the relentless environmental pressure of persistent heat.

**Table 2**
Daily Weather Conditions in Houston During the Study Period (July 1–14, 2024).

| Date | Max Temp (°F) | Min Temp (°F) | Heat Index (°F) | Notes |
|---|---|---|---|---|
| 2024-07-01 | 95 | 75 | 108 | Danger |
| 2024-07-02 | 95 | 79 | 110 | Danger |
| 2024-07-03 | 91 | 75 | 102 | Extreme Caution |
| 2024-07-04 | 88 | 77 | 99 | Extreme Caution |
| 2024-07-05 | 90 | 81 | 103 | Danger; High nighttime temperature |
| 2024-07-06 | 91 | 79 | 104 | Danger |
| 2024-07-07 | 90 | 79 | 105 | Danger |
| **2024-07-08** | **88** | **73** | **101** | **Extreme Caution; Hurricane Beryl Landfall / Outages begin** |
| 2024-07-09 | 88 | 75 | 100 | Extreme Caution; Widespread outages continue |
| 2024-07-10 | 91 | 77 | 104 | Danger; Widespread outages continue |
| 2024-07-11 | 93 | 79 | 108 | Danger; Widespread outages continue |
| 2024-07-12 | 93 | 81 | 109 | Danger; High nighttime temp; Outages |
| 2024-07-13 | 95 | 79 | 110 | Danger; Outages |
| 2024-07-14 | 93 | 77 | 107 | Danger; Outages |

This table displays daily maximum and minimum temperatures and the calculated maximum Heat Index for Houston. Risk classifications in the 'Notes' column follow U.S. National Weather Service (NWS) definitions, where a Heat Index of 90–103°F indicates 'Extreme Caution' and 103–124°F indicates 'Danger'.

### 3.6. Spatial lag regression

To account for spatial dependency in evacuation decisions, where neighboring communities influence local behavior, we employ a SLR model (Anselin, 1988; Pace and LeSage, 2009). In disaster research, this approach is critical since evacuation decisions depend not only on household factors but also on surrounding communities. The SLR model captures these spatial spillover effects by incorporating a spatially lagged dependent variable. Recent empirical research suggests that modeling spatial dependence improves accuracy. For instance, (Lindell and Perry, 2012), in the Protective Action Decision Model, highlighted that overlooking spatial interactions biased evacuation estimates. By integrating SLR, researchers can better understand how local interactions and socio-demographic factors jointly influence evacuation behavior, offering a more robust framework for policy and risk communication.

The model is specified by the following equation:

$$\mathbf{y} = \rho\mathbf{W}\mathbf{y} + \mathbf{X}\boldsymbol{\beta} + \boldsymbol{\epsilon} \tag{1}$$

where: $\mathbf{y}$ is a vector of the dependent variable, representing the evacuation rate for each community; $\rho$ is the spatial lag coefficient, which measures the strength of spatial dependence; $\mathbf{W}$ is the spatial weights matrix, defining the neighborhood structure between communities; $\mathbf{X}$ is a matrix of independent variables. Based on a comprehensive literature review, we selected 11 key factors for this study. These variables encompass (1) physical hazard exposure (power outage status, average surface temperature); (2) socioeconomic and resource variables (e.g., income, unemployment, vehicle ownership); and (3) demographic characteristics (e.g., age, disability, gender, race, single-parent status). $\boldsymbol{\beta}$ is a vector of coefficients for the independent variables; $\boldsymbol{\epsilon}$ is a vector of error terms.

Prior to fitting the SLR models, we conducted a multicollinearity diagnostic to ensure coefficient stability. Variance Inflation Factor (VIF) analysis revealed severe multicollinearity among ethno-racial composition variables: white ratio (VIF = 113.3), Hispanic ratio (VIF = 96.5), black ratio (VIF = 57.2), and Asian ratio (VIF = 13.6), all far exceeding the threshold of 10. To address this and create a more parsimonious model, we engineered a single variable, *percent minority*, defined as 1 minus the white ratio. The four original collinear race variables were removed, resolving multicollinearity and allowing reliable estimate of community racial composition effects.

### 3.7. Difference-in-differences model

Building on the spatial correlations identified earlier, we employ a DID model to estimate the causal impact of compound disaster exposure on daily evacuation behavior. We use a two-way fixed effects (TWFE) specification, which suits panel data by controlling for unobserved, time-invariant community characteristics and common shocks affecting all communities. Our empirical strategy is based on the following standard DID specification:

$$Y_{it} = \alpha_i + \lambda_t + \beta_1 \,\text{Treatment}_i \times \text{Post}_t + \epsilon_{it} \tag{2}$$

In this equation, the dependent variable, $Y_{it}$, represents calibrated daily evacuation rate for community $i$ on day $t$, derived by adjusting raw device counts with a blended penetration rate to better estimate the true population proportion. The model incorporates two-way fixed effects to: $\alpha_i$ represents community fixed effects, absorbing time-invariant local characteristics, while $\lambda_t$ denotes for time fixed effects, capturing common daily shocks. $\text{Treatment}_i$ identifies communities in the treatment or control group, while $\text{Post}_t$ denotes the post-event period. To handle partially affected areas, we apply the strict binary definition from Section 3.3. $\text{Treatment}_i = 1$ only for block groups with an aggregate NTL reduction above 15 units, indicating widespread power loss; otherwise $\text{Treatment}_i = 0$. This conservative rule ensures the treatment captures substantial infrastructure failure rather than localized noise. $\text{Post}_t$ is an indicator

equal to 1 for all days after the hurricane's landfall on July 8, and 0 for all days prior. The interaction of these terms allows us to estimate our primary coefficient of interest, $\beta_1$, which captures the average treatment effect on the treated (ATT). Finally, $\epsilon_{it}$ is the error term. This model exploits both cross-sectional variation between communities with and without power outages ($\text{Treatment}_i = 1$ vs. 0) and temporal variation before and after the event ($\text{Post}_t = 1$ vs. 0). The key identifying assumption is the parallel trends: absent the hurricane, evacuation trends in outage and non-outage communities would have evolved similarly.

Our coefficient of interest $\beta_1$ captures the DID interaction effect, estimating the additional change in evacuation rates attributable to outage in the post-disaster period. The TWFE DID framework is widely used in the climate and disaster economics for identifying causal impacts amid confounders (Carleton and Hsiang, 2016). Similar approaches evaluate the role of infrastructure like air conditioning in climate adaptation (Barreca et al., 2016) and behavioral responses to extreme weather (Burke and Emerick, 2016). To ensure the statistical validity, we cluster standard errors at the block-group level addressing serial correlation and producing reliable confidence intervals, as recommended by Bertrand et al. (2004). This robust framework allows us to move beyond simple correlation and draw credible, policy-relevant causal insights into evacuation dynamics under compound disasters.

### 3.8. Extreme gradient boosting with SHAP explanations

To capture non-linear and interaction-rich relationships between environmental stressors (heat, outage) and socio-demographic conditions, we employ XGBoost, a scalable gradient-boosted decision tree method with regularization that performs well on tabular data, tuned via spatially aware cross-validation. The target variable for the model is the log-transformed daily evacuation rate $\log(1 + Y_{it})$, which stabilizes variance and improves predictive performance for skewed mobility data. To ensure reproducibility and prevent overfitting due to spatial autocorrelation, we implemented a rigorous Spatial Cross-Validation (Spatial CV) strategy rather than a random train-test split. The dataset ($N = 2,042$ community-day observations) was divided into 5 spatially contiguous folds based on K-means clustering of geographic coordinates. In each iteration, the model was trained on 4 folds and validated on the remaining spatially distinct fold. Hyperparameters were tuned via Randomized Search within this spatial CV framework (300 iterations) to maximize the $R^2$ score.

We pair the trained model with SHAP to obtain both global (feature importance) and local (per-community, per-day) attributions that decompose each prediction into additive feature contributions. In contrast to traditional methods such as permutation importance or partial dependence plots, SHAP provides both global and local interpretability, allowing researchers to understand how individual variables affect specific predictions, which is crucial for personalized evacuation planning. This approach is conceptually based on the following additive feature attribution model:

$$g(\mathbf{z}') = \phi_0 + \sum_{i=1}^{M} \phi_i z_i' \tag{3}$$

where: $g$ is the explanation model; $\mathbf{z}'$ is a simplified binary input vector (1 if a feature is present, 0 if absent); $M$ is the number of input features; $\phi_i$ (phi) is the SHAP value (feature attribution) for feature $i$; $\phi_0$ is the base value (the prediction without any features).

We do not use XGBoost-SHAP to replace causal inference or spatial econometrics. Rather, we use it as a complementary heterogeneity analysis after SLR and DID have established, respectively, spatial dependence and average treatment effects. We considered transparent spatial statistical approaches such as (M)GWR. However, our objective is to characterize non-linear, interaction-driven mechanisms in a community-by-day panel setting, where standard GWR's locally linear specification and day-by-day bandwidth estimation can be unstable and difficult to interpret consistently. We therefore use SLR to address spatial dependence explicitly, and apply XGBoost with spatially aware cross-validation and SHAP explanations as a complementary approach to capture flexible, heterogeneous relationships while retaining interpretability at both global and local (community-day) scales. Prior to modeling, we examined multicollinearity among predictors using Variance Inflation Factors (VIF). This diagnostic revealed severe collinearity among the racial composition variables, which is expected given their compositional dependence. To reduce attribution instability in SHAP, we re-specified the model by removing the highly collinear race-share variables and retaining only one representative racial composition indicator. This XGBoost + SHAP workflow is increasingly applied in hazard and evacuation research. For instance, recent studies have used it to model flood susceptibility (Liu et al., 2025; Fu et al., 2025), landslide risks (Zhang et al., 2023), and urban flood depth prediction (Liu et al., 2025). The XGBoost and SHAP analyses were implemented in Python (version 3.11) using the scikit-learn (version 1.4.2) and shap (version 0.45.0) libraries.

## 4. Results

### 4.1. Evacuation decisions

Our analysis of evacuation patterns reveals a differentiated response between outage- and non-outage-affected communities during Hurricane Beryl. As shown in Fig. 3, both groups followed similar mobility patterns before landfall (July 1–7), with comparable average evacuation rates of 13.0% in non-outage areas and 12.4% in outage-affected areas across the Houston sample. However, following landfall on July 8, evacuation rates diverged. Communities that experienced power outages exhibited a sharper increase, peaking at around 20% on July 11, compared to approximately 16% in non-outage communities, and in the post-landfall period (July 8–14), the average evacuation rate in outage-affected areas rose to 15.7%, surpassing the 13.8% observed in non-outage areas. Communities classified as outage-affected did not exhibit an immediate surge in evacuations on July 9. Instead, evacuation rates rose

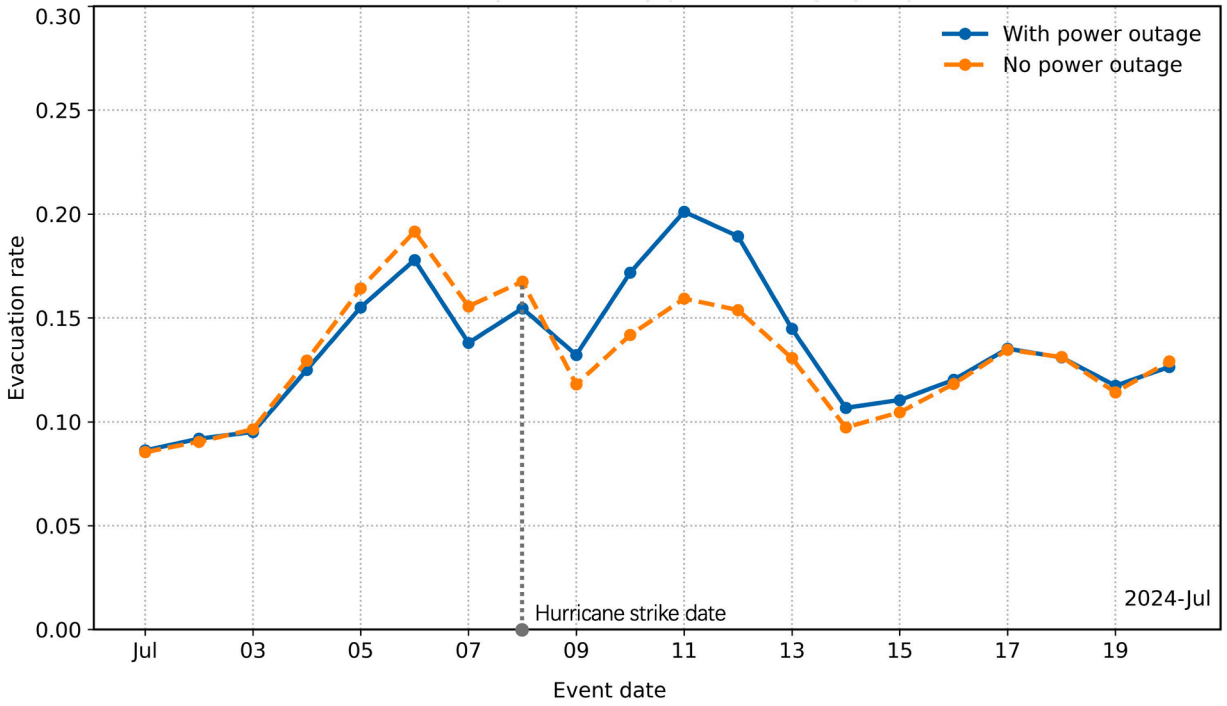


**Fig. 3.** Comparison of Evacuation Ratio and Heat Index Changes. The chart displays daily evacuation rates for communities with (blue) and without (orange) outages. The vertical dashed line indicates hurricane landfall (July 8). Outage-affected communities exhibited a sharper increase, peaking near 20% on July 11, versus approximately 16% in non-outage communities. (For interpretation of the references to colour in this figure legend, the reader is referred to the web version of this article.)

on July 10, and reached their peak on July 11. This delay suggests outages should not be interpreted simply as a proxy for storm-related housing damage; if widespread structural damage were the dominant driver, departures would likely have peaked immediately following landfall. Rather, the lag reflects cumulative stress: prolonged electricity loss under extreme heat progressively eroded households' capacity to shelter in place, prompting larger-scale departures by July 11. Storm-related housing damage, however, may still have contributed. Overall, the short-term displacement in outage-affected communities reinforces the critical role of infrastructure resilience in shaping protective behavior under compound disasters.

Extending the temporal analysis, the spatial distribution further underscores the complexity of household responses under compound hazards. As shown in Fig. 4a–c, evacuation was spatially clustered, with certain suburban corridors showing consistently higher outflows. Strikingly, these clusters did not align with the areas that experiencing the most severe blackouts (Fig. 2), producing a spatial mismatch between exposure and response. This suggests, consistent with prior literature, that evacuation is strongly shaped by socioeconomic constraints. Communities facing the greatest compounded risks were not always those most able to leave. Such spatial dependencies motivate SLR to quantify correlation and spillover. Yet correlation alone does not establish causality, motivating the use of DID models to isolate the causal effects of outages under extreme heat. Finally, because DID estimates average effects but not heterogeneous mechanisms, we employ machine-learning to capture variation across communities. Together, this multi-stage design connects temporal dynamics with spatial heterogeneity, providing a robust basis for causal inference and mechanism exploration.

### *4.2. Social vulnerability*

To formally test our hypotheses and identify community-level drivers of evacuation, we employed the SLR model. This approach tests and controls for spatial spillover effects, addressing our third hypothesis (H3) on spatial dependence. The model quantifies the influence of socioeconomic factors on evacuation likelihood, thereby also testing delayed evacuation (H1) and social vulnerability (H2).

In the SLR analysis of evacuation rates before (pre-outage) and after (post-outage) the hurricane, we observed notable changes and commonalities. In Table 3, arrows indicate coefficient changes between the two periods (↑ for increase, ↓ for decrease, and ~ for stability). First, both models demonstrate reasonable explanatory power, with pseudo $R^2$ values of 0.315 (pre-outage) and 0.288 (post-outage). The spatial lag term ($W$) is highly significant in both periods ($p < .001$), confirming strong spatial dependence. In other words, community decisions to evacuate WERE influenced by neighboring areas, underscoring spatial spillovers under compound hazards, which supports our third hypothesis (H3) regarding spatial dependence.

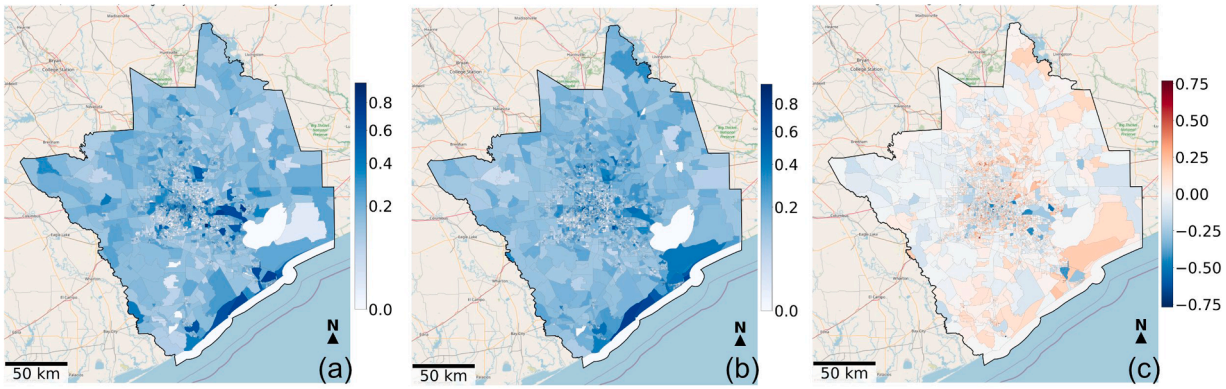


**Fig. 4.** The evacuation origins before and after the power outage in Houston MSA. (a) Evacuation rate of origins during the pre-disaster phase (July 1–7). (b) Evacuation rate of origins during the post-disaster phase (July 8–14). (c) The change in average daily evacuation rate between the two phases (Phase 2 minus Phase 1), where blue indicates a decrease and red indicates an increase. The maps reveal that the communities with the largest increase in post-disaster evacuations did not directly align with those that experienced power outages, suggesting a complex set of influencing factors. (For interpretation of the references to colour in this figure legend, the reader is referred to the web version of this article.)

**Table 3**
SLR Results in Pre-Outage and Post-Outage Periods.

| Variable | Pre-Outage Coeff. | Post-Outage Coeff. | Pre-Outage *p*-Value | Post-Outage *p*-Value |
|---|---|---|---|---|
| **Spatial lag term ($W$)** | **0.468** | **0.438** ↓ | **<0.001** | **<0.001** |
| **Hazard Exposure** | | | | |
| Power outage | −0.039 | 0.013 ↑ | < 0.001 | 0.007 |
| **Geographic Controls** | | | | |
| Distance to coastline | 0.009 | 0.001 ↓ | 0.179 | 0.935 |
| Distance to nearest highway | −0.007 | −0.002 ↑ | 0.349 | 0.772 |
| **Socioeconomic & Demographics** | | | | |
| Population > 65 Ratio | −0.007 | −0.004 ↑ | 0.423 | 0.65 |
| Population < 17 Ratio | 0.001 | −0.001 ↓ | 0.887 | 0.881 |
| **Unemployment Rate** | **−0.021** | **−0.007** ↑ | **0.006** | **0.405** |
| Poverty Rate | −0.008 | 0.002 ↑ | 0.371 | 0.809 |
| **Percent Minority** | **−0.044** | **−0.044** ∼ | **< 0.001** | **< 0.001** |
| Vehicles per Household | −0.035 | −0.021 ↑ | < 0.001 | 0.028 |
| Median Household Income | 0.016 | 0.001 ↓ | 0.091 | 0.913 |
| Number of Households | −0.027 | −0.013 ↑ | < 0.001 | 0.102 |
| Male to Female Ratio | −0.004 | −0.002 ↑ | 0.517 | 0.814 |
| **Single Parent Ratio** | **−0.046** | **−0.026** ↑ | **< 0.001** | **0.003** |
| Disability Ratio | −0.018 | 0.007 ↑ | 0.034 | 0.409 |
| No Vehicle Rate | 0.000 | −0.003 ↓ | 0.970 | 0.774 |
| **Population density** | **−0.082** | **−0.034** ↓ | **< 0.001** | **< 0.001** |
| Pseudo $R^2$ | Pre-Outage: 0.315 | Post-Outage: 0.288 | | |

This table presents coefficients and *p*-values from two separate SLR examining determinants of community evacuation rates during the Pre-Outage and Post-Outage periods. The dependent variable is the daily community evacuation rate. Arrows in the "Post-Outage Coeff." column indicate coefficient changes relative to the pre-outage period (↑ for an algebraic increase, ↓ for a decrease, and ∼ for relative stability).

The findings also support Hypothesis 1, which proposed that the compound hazard of power outages and extreme heat would trigger delayed evacuations. A comparison of the coefficients before and after the outage reveals both commonalities and important shifts. Regarding hazard and geographic exposure, the direct effect of power outage shows a dramatic reversal. In the pre-outage period, communities designated with future power outages had a significantly lower propensity to evacuate (coefficient = −0.039, $p < .001$), suggesting structural barriers to mobility. However, in the post-outage period, the effect flips, with power loss becoming a positive, borderline-significant driver of evacuations (coefficient = 0.013, $p = .097$). This indicates that while initial evacuations were lower in at-risk areas, actual outages triggered later departures. In contrast, factors like distance to the coastline and proximity to highways were not statistically significant once controls were added.

The results also validate Hypothesis 2, that post-landfall evacuees disproportionately come from socially vulnerable communities. Across both periods, key vulnerability indicators were negative predictors: population density (coefficients −0.082 and −0.035), percent minority (both −0.044), single-parent households (−0.046 and −0.026), and vehicles per household (−0.035 and −0.021), all highly significant predictors across both phases. Some vulnerabilities shifted as the crisis evolved. Unemployment rate (−0.021, $p < .01$) and the disability ratio (−0.018, $p < .05$) were significant barriers only before landfall, losing significance after the outage, suggesting these

**Table 4**
DID Results.

| Variable / Interaction | Coefficient | Std. Error | $z/t$ | $p$-value | 95% CI |
|---|---|---|---|---|---|
| Outage × Post (ATT) | +0.030 | 0.0035 | 8.69 | < 0.001 | [0.023, 0.037] |

The dependent variable is the daily calibrated community evacuation rate. The model includes community and day fixed effects, with standard errors clustered at the community level ($N$ = 34,959 community-day observations across 2928 block groups and 12 days).

factors constrain proactive evacuations but become less distinct once disruption occurs. By contrast, age composition and poverty rates were not consistently significant.

Taken together, the SLR results reveal a complex picture: evacuation is shaped by spatial spillovers, but socioeconomic vulnerability remains the most consistent barrier with effects often stronger under compounded stress. However, spatial correlation does not by itself establish causality. To move beyond associations and to isolate the causal impact of outages under extreme heat, we next turn to a DID framework.

### 4.3. Causal effects of compound exposure

Building on the spatial correlation identified in the SLR, we next employed a two-way fixed effects (TWFE) DID model to isolate the causal impact of outages. Table 4 reports the key coefficients. The model includes community and date fixed effects, with standard errors clustered at the community level.

The estimated ATT of +0.030 indicates that, net of community and day fixed effects, daily evacuation rates in outage-affected communities were on average 3.0 percentage points higher than in non-outage communities throughout the post-landfall period, a 22% increase relative to the 13.7% pre-landfall mean in treated communities. This positive effect provides causal evidence that the cascading failure of power infrastructure under extreme heat actively pushed households out of their homes, supporting our hypothesis (H1) that compound hazards trigger a delayed wave of evacuation as worsening indoor conditions erode the feasibility of sheltering in place.

To probe the temporal structure of this effect and to assess the parallel-trends assumption, we estimated the corresponding event-study specification. Fig. 5 plots the relative-time coefficients $\beta_k$ for $k \in \{-5, \ldots, +5\}$, with $k = -1$ (July 7) as the omitted reference period.

The dynamic estimates support a delayed-evacuation interpretation in three ways. First, the four pre-landfall coefficients are small in magnitude and decline monotonically toward zero as landfall approaches: $\beta_{-5} = +0.019$, $\beta_{-4} = +0.014$, $\beta_{-3} = +0.011$, $\beta_{-2} = +0.002$. The latter two coefficients are statistically indistinguishable from the omitted reference period at conventional levels ($p = .054$ and $p = .72$, respectively). The slight elevation observed at $k = -5$ and $k = -4$ likely reflects modest geographically-correlated anticipatory behavior in outage-prone, low-lying communities once official hurricane warnings were issued for the Texas coast. On the day of landfall itself ($\beta_0 = +0.009$), the response is essentially zero. The differential evacuation only emerges from $k = +1$ onward, peaks at $\beta_{+3} = +0.061$ on July 11, exactly three days after the onset of widespread outages, and partially attenuates by $k = +5$. This 2–3 day lag is incompatible with an interpretation in which outage and evacuation are coincident manifestations of hurricane impact, and is precisely the pattern predicted by a mechanism in which prolonged power loss under extreme heat progressively erodes households' capacity to shelter in place.

As a robustness check against the modest pre-trend drift visible at $k \leq -3$, we re-estimated the static DID on a restricted window covering only $k \in [-2, +5]$ (July 6–13), over which pre-trends are flat. The restricted-window ATT is +0.039 (SE 0.0046, $p < .001$, $N$ = 23,342), slightly larger than the full-window estimate, indicating that the small anticipatory drift at $k \leq -3$ if anything attenuates rather than inflates our main effect. The point estimate from a permutation placebo test (Appendix A.2) on the peak-effect day (July 11) further confirms that the observed outage–non-outage gap is far larger than what arbitrary spatial reassignment of the outage label can produce ($p < .001$).

While DID provides robust evidence of the average causal effect of outages, it does not reveal which communities were most constrained or most responsive. To uncover these heterogeneous mechanisms and identify the most affected social groups, we next employ machine-learning models with SHAP-based interpretation.

### 4.4. Heterogeneous effects and machine learning insights

While the SLR analysis provided spatial dependence and socioeconomic correlations, and the DID framework identified average causal effects of outages under extreme heat, these approaches do not reveal which communities were most affected. To address this, we employed an XGBoost model with SHAP interpretation to explore heterogeneous effects across community characteristics. The model achieved solid predictive performance ($R^2 = 0.524 \pm 0.042$; RMSE = 1.08; MAE = 0.66), demonstrating its ability to capture complex, nonlinear relationships in evacuation dynamics.

The SHAP importance ranking (Fig. 6a) highlights population density and racial composition as the most influential predictors, consistent with regression results. Vehicle availability and spatial variables, such as distance to the coastline, also emerged as highly

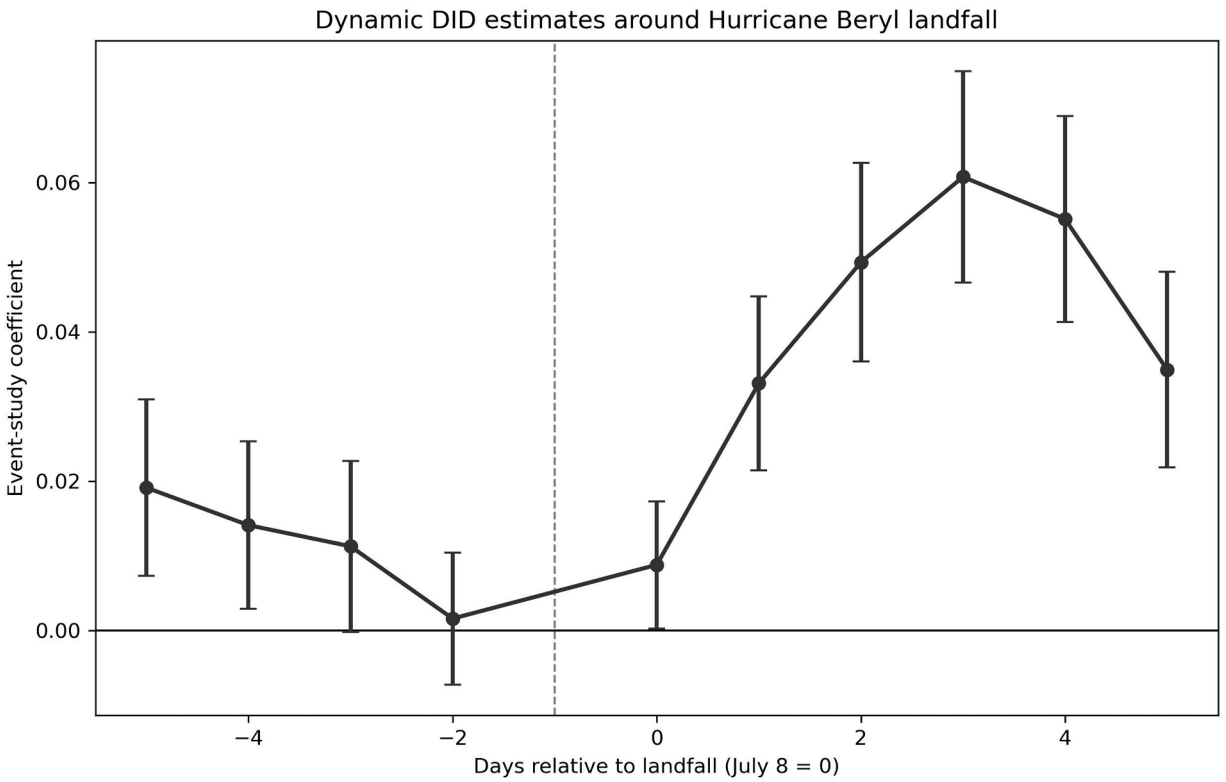


**Fig. 5.** Event-study DID estimates around Hurricane Beryl landfall. Points show coefficients $\beta_k$ from a TWFE specification with relative-time dummies interacted with the outage indicator, using $k = -1$ (July 7) as the omitted reference period. Error bars denote 95% confidence intervals based on cluster-robust standard errors. The vertical dashed line marks landfall.

relevant. The SHAP beeswarm plot (Fig. 6b) further reveals the direction and distribution of feature effects. Constraint-related features such as population density, single-parent ratio, and poverty rate exerted consistently negative effects: high values (red points) are concentrated on the negative side of the SHAP axis, indicating that dense, socioeconomically vulnerable communities were less likely to evacuate. In contrast, White population was a strong positive predictor, with high values (red points) clustered on the positive side, signaling greater evacuation capacity. Counterintuitively, Vehicle Per Household also emerges as a negative predictor, with higher values associated with lower evacuation rates. Spatial exposure variables, including distance to the coastline, showed complex, nonlinear effects, with coastal proximity generally raising evacuation propensity but with substantial variation across communities. Notably, outage-related interactions (e.g., outage × no vehicle, outage × poverty) cluster around negative SHAP contributions, confirming that when outages overlapped with limited mobility, dependency, or financial disadvantage, evacuation rates were further suppressed. Temporal controls and temperature variables exhibit limited impact, as common shocks were absorbed by the DID fixed-effects. Together, the beeswarm analysis reinforces and extends regression findings by showing not only which variables matter most but also how their effects differ across communities, highlighting the compounded vulnerability of high-density, mobility-constrained, and socially dependent groups under blackout and heat stress.

Beyond global importance, SHAP interaction analyses and stratified heterogeneity plots (Fig. 7) reveal distinct vulnerability profiles. Communities with higher residents with disabilities, households without vehicles, or higher poverty rates consistently faced disproportionately negative impacts of outages, with predicted evacuation deficits reaching −0.02 to −0.035 relative to non-outage communities. In contrast, elderly populations (65 + ) showed a more complex pattern: deficits were notable in moderately aged communities (Q2–Q3) but weaker in the highest-aging quartile (Q4), likely reflecting “trapped” populations unable to leave at all. These findings underline that evacuation barriers are not evenly distributed but clustered among specific vulnerable groups, particularly those with mobility and economic constraints.

In sum, the machine-learning results extend the DID by uncovering heterogeneity in outage effects. While the average effect of outages is to increase evacuation after landfall, this increase is unevenly distributed and substantially muted in communities marked by low mobility capacity, high dependency, and structural socioeconomic disadvantage.

## 5. Discussion

Our findings reveal a more differentiated relationship between compound hazards and evacuation than is assumed in conventional disaster models. On average, the DID results show that prolonged outages under extreme heat did eventually trigger a delayed increase

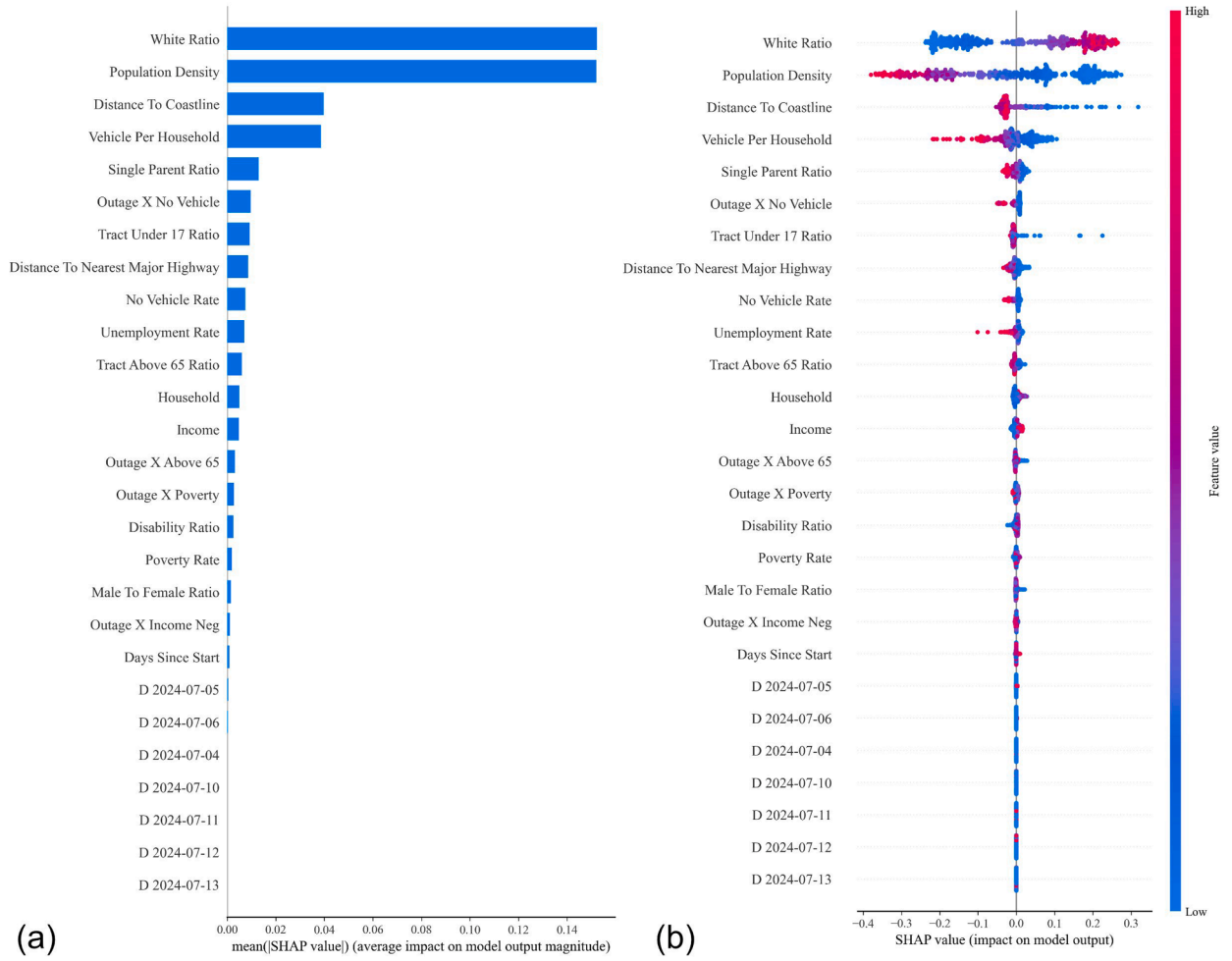


**Fig. 6.** SHAP importance ranking and beeswarm plot. (a) The importance ranking shows the average impact of each variable, with population density and racial composition emerging as the strongest predictors. (b) The beeswarm plot visualizes the direction and distribution of effects: each point represents a community, with colors indicating feature values (red = high, blue = low) and position on the $x$-axis indicating whether the factor increases (right) or decreases (left) evacuation likelihood. Constraint-related features (e.g., population density) cluster negatively, while enabling factors (e.g., White ratio) cluster positively, confirming systematic disparities in evacuation capacity. (For interpretation of the references to colour in this figure legend, the reader is referred to the web version of this article.)

in evacuation, indicating that worsening post-landfall conditions did push some households to leave. Furthermore, the descriptive patterns, spatial analysis, and XGBoost-SHAP results show that this response was far from uniform: communities marked by greater social vulnerability were less able to translate escalating risk into timely evacuation. This finding both extends and qualifies classic frameworks such as the Protective Action Decision Model (PADM), which emphasizes that stronger risk perception and protective action efficacy increase the likelihood of evacuation (Lindell and Perry, 2012). Our results suggest that, under compound hazards, these mechanisms remain important but are not sufficient. Cascading infrastructural failure can erode the practical capacity to act, even when risk is recognized. In this sense, the issue is not simply whether people perceive danger, but whether they retain the material means to respond to it. A widespread power outage can remove cooling, disrupt information access, increase financial strain, and thereby constrain evacuation options, especially for already disadvantaged households. For instance, after Hurricane Sandy, (Carbone and Wright, 2016) documented how elderly residents were left unable to evacuate from powerless buildings. Such paralysis has been theorized in climate mobility literature. (Black and Collyer, 2014) warned of “trapped populations” who are unable to flee high-risk areas due to resource constraints. Our study provides tangible evidence: power loss and poverty combined to trap populations despite escalating danger. Compared with rapid-onset events such as wildfires, where visible and immediate danger often prompts swift evacuation (Synolakis and Karagiannis, 2024), the post-hurricane combination of blackout and heat appears to produce a slower and more uneven response, in which action is postponed and the burden of waiting is distributed unequally across communities.

Second, our analysis quantifies how pre-existing social inequalities shape evacuation behavior under compound events, reinforcing and extending the literature on environmental justice and disaster disparities. Communities with higher socioeconomic advantages—for example, those with higher incomes, vehicle ownership, and majority-white populations—exhibited greater evacuation rates.

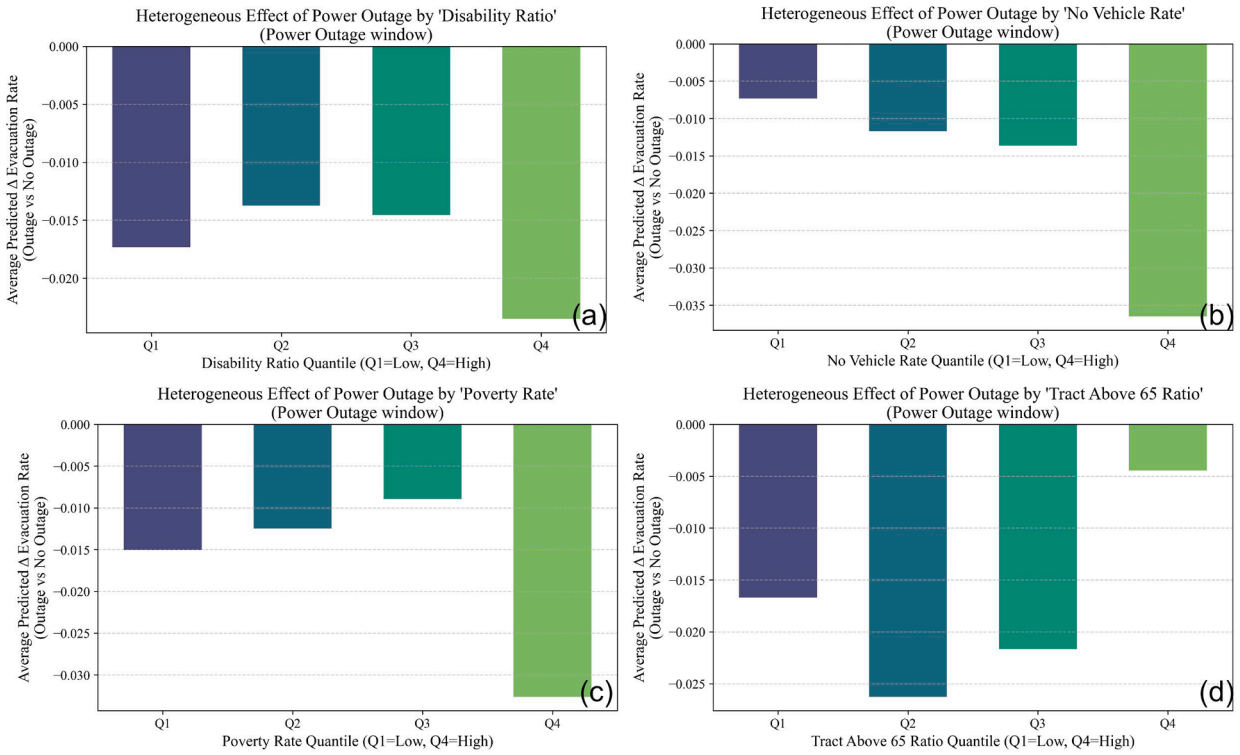


**Fig. 7.** Heterogeneous effects of power outages on evacuation under high-heat conditions. (a) Disability ratio, (b) no-vehicle households, (c) poverty rate, and (d) elderly population (65 +) are stratified into quartiles (Q1 = lowest, Q4 = highest). Bars show the average predicted difference in evacuation rates between outage and non-outage communities. Higher disability, no-vehicle, or poverty levels show systematically larger evacuation deficits, underscoring mobility and resource barriers. The elderly dimension exhibits a nonlinear pattern, with stronger deficits in moderately aged communities (Q2–Q3) but weaker effects in the highest-aging quartile (Q4), possibly indicating trapped populations unable to evacuate.

This aligns with extensive research showing that socially vulnerable groups are less able or willing to evacuate (Coleman et al., 2020; Karakoc et al., 2020; Mitsova et al., 2018; Rodriguez et al., 2022; Rodríguez-Avellaneda et al., 2025; Stough et al., 2016). Our finding that white-majority neighborhoods evacuated at higher rates echoes prior studies. After Hurricane Katrina, (Fussell et al., 2010) found that Black residents were significantly less likely than white residents to evacuate, due to lower vehicle ownership, financial constraints, and distrust of institutions. More recent mobility studies confirm that racial minorities and low-income households evacuate less than wealthier white residents (Yabe et al., 2020; Deng et al., 2021). Our study builds on this literature by demonstrating these disparities in real time during a compound hazard. These findings reinforce the concept of "mobility justice": the ability to move to safety is not just about risk awareness, but fundamentally about having access to resources and infrastructure (Sheller, 2018). In sum, socioeconomic factors in our models underscore how social vulnerability remains the most consistent predictor of disaster outcomes. We extend prior environmental justice research by showing that these well-known disparities not only persist but may widen during multi-hazard crises.

Third, our results contribute new evidence on the spatial dynamics of evacuation under compound hazards. We found strong spatial autocorrelation in evacuation rates, suggesting spillovers likely driven by social networks and local information sharing, aligns with earlier work on network effects (Hasan and Ukkusuri, 2011). In our case, neighbors leaving or discussing worsening conditions likely created contagious evacuation effect. A novel observation, however, was that although outage-affected communities on average evacuated more after landfall, the spatial pattern of evacuation did not align cleanly with the most severely impacted areas: vulnerable subsets within outage zones lagged substantially behind, producing a within-treatment mismatch between exposure and response. We quantitatively captured this mismatch in our compound hazard scenario, providing systematic evidence of what has been qualitatively observed in past disasters. This highlights the need for spatially targeted analysis to identify where high hazard does not translate to high response. We responded to this by employing a DID design with community fixed effects, ensuring that causal estimates reflected within-community changes due to outages and heat, separate from any static spatial factors.

Finally, by leveraging a two-stage analytical approach (causal inference followed by machine-learning interpretation), our study offers insights into the mechanisms behind the average effects. The DID results established the average causal impact of compound exposure. However, the DID alone cannot tell us who exactly bore this effect most strongly. To address this, we trained an XGBoost model and used SHAP values to diagnose which community features were most associated with evacuation deficits. This approach responds to recent calls in the social sciences to move beyond average treatment effects and explore heterogeneous effects, using machine-learning as a tool for causal discovery (Athey and Imbens, 2017). The machine-learning interpretation confirmed and deep-

ened the regression findings. Our study is among the first to quantitatively isolate compounded vulnerabilities with a data-driven approach. While traditional regression use pre-specified interaction terms to probe heterogeneity, the SHAP framework allows more flexible, data-driven exploration of high-order interactions and non-linear relationships that are difficult to model explicitly (Lundberg and Lee, 2017). This provides a more granular understanding of vulnerability, pinpointing not just which groups are at risk but how multiple risk factors combine to produce acute outcomes. Such information can guide authorities to target outreach or assistance with much higher precision.

## 6. Conclusion

This study examined evacuation behavior during Hurricane Beryl in Houston under the compound stressors of widespread power outages and extreme heat. The key contribution is a nuanced understanding of how compounding risks alter evacuation dynamics and exacerbate social inequalities. Empirically, we show that socioeconomic vulnerability (poverty, minority status, age, disability) strongly constrained those who evacuated, highlighting profound evacuation disparities. We also document a delayed but significant surge in evacuations triggered by prolonged outages and heat, a two-phase pattern not captured in traditional single-hazard studies. Methodologically, we integrate high-resolution mobility data with spatial-DID causal inference and SHAP-based model interpretation, offering a novel approach to disentangle evacuation drivers. Collectively, these findings advance evacuation research by illuminating the interplay between social vulnerability, network effects, and multi-hazard stress through a state-of-the-art analytical lens.

Moving forward, the evidence urges a shift toward equity-centered, compound-risk-responsive planning. First, regarding mobility, plans should provide targeted evacuation support for low-vehicle-access communities through pre-positioned municipal transport fleets, reducing the logistical barriers to exit. Second, to support timely and equitable evacuation under cascading power loss and heat, authorities should establish accessible cooling and charging centers equipped with backup generators in underserved neighborhoods. Third, recovery strategies need to rethink grid restoration prioritization: rather than solely optimizing for the speed of reconnection or commercial value, restoration sequences should explicitly weigh social vulnerability to ensure life-sustaining power reaches at-risk populations faster. In summary, effective evacuation is not merely individual choice under risk but a systemic outcome shaped by inequities and concurrent dangers. Addressing these challenges requires reimagining protocols through the dual lenses of justice and multi-hazard resilience, ensuring that as disasters grow more complex, responses remain inclusive, adaptive, and lifesaving.

It is also important to acknowledge the limitations of this study. First is the representativeness of the mobile device dataset. While not a probability sample, mobility data have been shown to reliably reproduce aggregate travel patterns at metropolitan scales (Lu et al., 2017; Sinclair et al., 2023). Still, the sample may underrepresent groups with limited smart device usage, such as the very young, elderly, or low-income residents. Our analysis excludes individuals without smart devices or who did not opt in, who may disproportionately include vulnerable groups. These conditions may systematically underrepresent groups with lower smart device access or more unstable digital connectivity, including some elderly, low-income, and otherwise vulnerable residents. In a compound disaster context, this bias may be further amplified if severe outages reduce device charging or data generation precisely in the communities most at risk. Accordingly, our estimates likely capture behavioral patterns among observed device users rather than the full population, and the magnitude of evacuation inequality may be conservative if the most constrained residents are also the least observable in the data. Second, our use of aggregated socioeconomic data from the ACS has inherent ecological limitations, as community-level measures do not necessarily apply to each resident. Furthermore, our NTL analysis relied on single-date, clear-sky images due to cloud cover, which may add noise compared with multi-day composite. Third, our Land Surface Temperature (LST) data capture relative heat patterns but are not a direct substitute for near-surface air temperature, possibly under- or over-estimation of absolute thermal stress, though still valuable for assessing spatial disparities. Besides, our findings are based on a single case study in Houston, and their generalizability to other regions or hazards requires further investigation. Finally, while mobile device data reveal behavioral patterns, they cannot explain underlying motivations (e.g., financial barriers vs. lack of information), which future qualitative work could address.

Future research could pursue longitudinal studies on the long-term effects of compound disasters and policy interventions on vulnerable populations, broaden geographic and hazard contexts (e.g., wildfires with hazardous air pollution) to assess generalizability, and expand behavioral analyses with real-time data analytics to enhance predictive models and inform more adaptive emergency response strategies.

## CRediT authorship contribution statement

**Xin Wang:** Conceptualization, Visualization, Writing – original draft, Writing – review & editing; **Wei Zhai:** Conceptualization, Data curation, Formal analysis, Writing – review & editing; **Kerry Nice:** Writing – review & editing; **Benteng Sun:** Conceptualization, Writing – review & editing; **Xueyin Bai:** Conceptualization, Writing – review & editing; **Haoming Qin:** Data curation, Formal analysis; **Huanchun Huang:** Data curation, Conceptualization.

## Data availability

The authors do not have permission to share data.

## Declaration of competing interest

None

## Appendix A. Robustness cecks

### A.1. Sensitivity to evacuation threshold

Figs. A.1 and A.2.

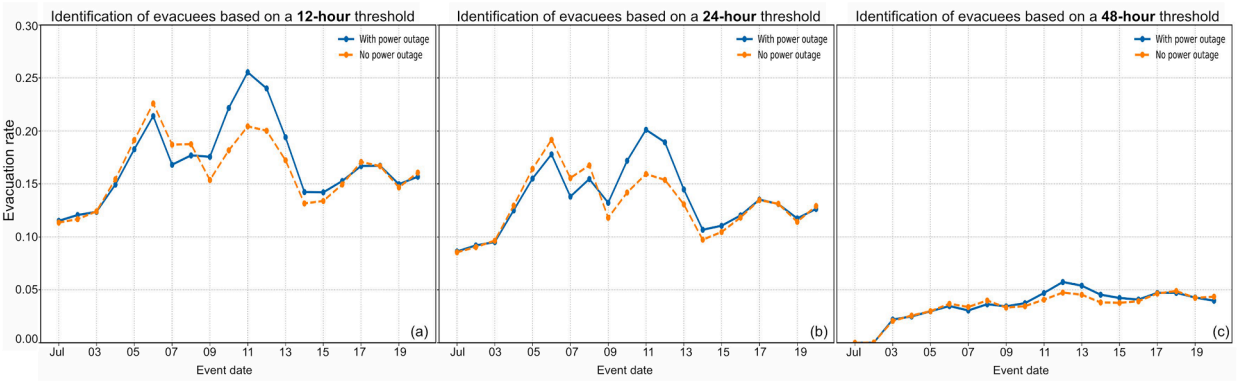


**Fig. A.1.** Identification of evacuees based on alternative time thresholds. (a) 12-hour threshold, (b) 24-hour threshold, and (c) 48-hour threshold. All three thresholds show consistent temporal dynamics in the outage gap, with the daily difference between outage and non-outage communities correlated at $r = 0.991$ between the 12-hour and 24-hour definitions and at $r = 0.785$ between the 24-hour and 48-hour definitions. The 24-hour threshold provides the most robust balance between filtering routine travel and capturing diverse evacuation behaviors.

### A.2. Permutation placebo test

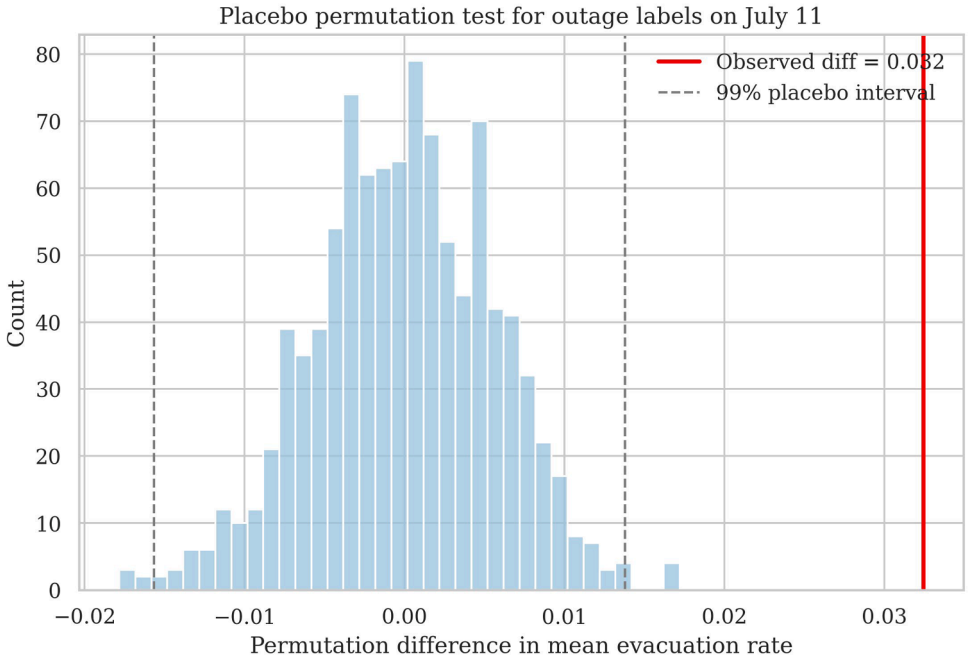


**Fig. A.2.** Placebo permutation test for outage labels on July 11. The histogram shows the distribution of permutation differences in mean evacuation rate across 1000 random reassignments of the binary outage label. The red vertical line indicates the observed difference of 0.032, which lies far outside the 99% placebo interval (dashed lines) of $[-0.0157, 0.0138]$. The empirical $p$-value is below 0.001, confirming that the measured outage–non-outage gap cannot be reproduced by arbitrary spatial assignment. (For interpretation of the references to colour in this figure legend, the reader is referred to the web version of this article.)

## References


Adeola, F.O., Picou, J.S., 2016. Hurricane Katrina-linked environmental injustice: race, class, and place differentials in attitudes. Disasters 41 (2), 228–257 , https://doi.org/10.1111/disa.12204.

Alemazkoor, N., Rachunok, B., Chavas, D.R., Staid, A., Louhghalam, A., Nateghi, R., Tootkaboni, M., 2020. Hurricane-induced power outage risk under climate change is primarily driven by the uncertainty in projections of future hurricane frequency. Sci. Rep. 10(1), https://doi.org/10.1038/s41598-020-72207-z.

Anselin, L., 1988. Spatial Econometrics: Methods and Models. Kluwer Academic Publishers.

Anyidoho, P.K., Ju, X., Davidson, R.A., et al., 2023. A machine learning approach for predicting hurricane evacuee destination location using smartphone location data. Comput. Urban Sci. 3 (30). https://doi.org/10.1007/s43762-023-00102-0.

Athey, S., Imbens, G.W., 2017. The state of applied econometrics: causality and policy evaluation. J. Econ. Perspect. 31 (2), 3–32. https://doi.org/10.1257/jep.31.2.3.

Barreca, A., Clay, K., Deschenes, O., Greenstone, M., Shapiro, J.S., 2016. Adapting to climate change: the remarkable decline in the US temperature-mortality relationship over the twentieth century. J. Polit. Econ. 124 (1), 105–159.

Bertrand, M., Duflo, E., Mullainathan, S., 2004. How much should we trust differences-in-differences estimates?. Q. J. Econ. 119 (1), 249–275.

Black, R., Collyer, M., 2014. Populations 'trapped' at times of crisis. Forced Migr. Rev. 45, 52–54.

Best, K., Kerr, S.E., Reilly, A., Patwardhan, A., Niemeier, D., Guikema, S.D., 2022. Spatial regression identifies socioeconomic inequality in multi-stage power outage recovery after hurricane isaac. Res. Sq. https://doi.org/10.21203/rs.3.rs-2113226/v1.

Bolin, B., Kurtz, L.C., 2017. Race, class, ethnicity, and disaster vulnerability. Handb. Disaster Res., 181–203. https://doi.org/10.1007/978-3-319-63254-4_10.

Burke, M., Emerick, K., 2016. Adaptation to climate change: evidence from US agriculture. Am. Econ. J. Econ. Policy 8 (3), 106–140.

Carbone, E.G., Wright, M.M., 2016. Hurricane Sandy recovery science: a model for disaster research. Disaster Med. Public Health Prep. 10 (3), 304–305. https://doi.org/10.1017/dmp.2015.140.

Carleton, T.A., Hsiang, S.M., 2016. Social and economic impacts of climate. Science 353 (6304), aad9837.

Cheng, H., 2021. Hurricane evacuation behavior analysis based on mobile location data: a case study of Hurricane Florence. Cornell University eCommons. https://doi.org/10.7298/nem7-gf83.

CNN, 2023. Extreme heat is the deadliest natural disaster. FEMA can't treat it like one. https://www.cnn.com/2023/08/08/politics/heat-fema-federal-response-biden-climate/index.html.

Coleman, N., Esmalian, A., Mostafavi, A., 2020. Equitable resilience in infrastructure systems: empirical assessment of disparities in hardship experiences of vulnerable populations during service disruptions. Nat. Hazards Rev. 21 (4), 4020034. https://doi.org/10.1061/(ASCE)NH.1527-6996.0000401.

Coleman, N., Liu, C., Zhao, Y., Mostafavi, A., 2023. Lifestyle pattern analysis unveils recovery trajectories of communities impacted by disasters. Humanit. Soc. Sci. Commun. 10 (1), 1–13 , https://doi.org/10.1057/s41599-023-02312-7.

Dance, S., 2024. After Beryl, power outages could last a week or more for 350,000 Texans https://www.washingtonpost.com/weather/2024/07/11/hurricane-beryl-texas-power-outages.

Deng, H., Aldrich, D.P., Danziger, M.M., Gao, J., Phillips, N.E., Cornelius, S.P., Wang, Q.R., 2021. High-resolution human mobility data reveal race and wealth disparities in disaster evacuation patterns. Humanit. Soc. Sci. Commun. 8 (1). https://doi.org/10.1057/s41599-021-00824-8.

Ebi, K.L., Capon, A., Berry, P., Broderick, C., de Dear, R., Havenith, G., …, Jay, O., 2021. Hot weather and heat extremes: health risks. Lancet 398 (10301), 698–708. https://doi.org/10.1016/s0140-6736(21)01208-3.

Feng, K., Lin, N., 2022. Modeling and analyzing the traffic flow during evacuation in Hurricane Irma (2017). Transp. Res. D Transp. Environ. 110, 103412. https://doi.org/10.1016/j.trd.2022.103412.

Feng, K., Ouyang, M., Lin, N., 2022. Tropical cyclone-blackout-heatwave compound hazard resilience in a changing climate. Nat. Commun. 13 (1), 4421. https://doi.org/10.1038/s41467-022-32018-4.

Flanagan, B.E., Gregory, E.W., Hallisey, E.J., Heitgerd, J.L., Lewis, B., 2011. A social vulnerability index for disaster management. J. Homel. Secur. Emerg. Manag. 8 (1).

Fu, X., Wang, M., Zhang, D., Chen, F., Peng, X., Wang, L., Tan, S.K., 2025. An XGBoost-SHAP framework for identifying key drivers of urban flooding and developing targeted mitigation strategies. Ecol. Indic. 175, 113579. https://doi.org/10.1016/j.ecolind.2025.113579.

Fussell, E., Sastry, N., VanLandingham, M., 2010. Race, socioeconomic status, and return migration to New Orleans after Hurricane Katrina. Popul. Environ. 31 (1–3), 20–42. https://doi.org/10.1007/s11111-009-0092-2.

Gori, A., Lin, N., Xi, D., Emanuel, K., 2022. Tropical cyclone climatology change greatly exacerbates US extreme rainfall–surge hazard. Nat. Clim. Change 12 (2), 171–178. https://doi.org/10.1038/s41558-021-01272-7.

Gould, C.F., Heft-Neal, S., Johnson, M., Aguilera, J., Burke, M., Nadeau, K., 2024. Health effects of wildfire smoke exposure. Annu. Rev. Med. 75, 277–292. https://doi.org/10.1146/annurev-med-052422-020909.

Gu, X., Chen, P., Fan, C., 2024. Socio-demographic inequalities in the impacts of extreme temperatures on population mobility. J. Transp. Geogr. 114, 103755. https://doi.org/10.1016/j.jtrangeo.2023.103755.

Hasan, S., Ukkusuri, S.V., 2011. A threshold model of social contagion process for evacuation decision making. Transp. Res. B Methodol. 45 (10), 1590–1605. https://doi.org/10.1016/j.trb.2011.07.008.

Hong, B., Bonczak, B.J., Gupta, A., Kontokosta, C.E., 2021. Measuring inequality in community resilience to natural disasters using large-scale mobility data. Nat. Commun. 12 (1), https://doi.org/10.1038/s41467-021-22160-w.

Houston, J.B., Hawthorne, J., Perreault, M.F., Park, E.H., Goldstein Hode, M., Halliwell, M.R., …, Griffith, S.A., 2014. Social media and disasters: a functional framework for social media use in disaster planning, response, and research. Disasters 39 (1), 1–22. https://doi.org/10.1111/disa.12092.

Houston Public Media, 2024. Hurricane Beryl heat-related fatalities in Houston rise to 40. https://www.houstonpublicmedia.org.

Howe, P.D., Marlon, J.R., Wang, X., Leiserowitz, A., 2019. Public perceptions of the health risks of extreme heat across U.S. states, counties, and neighborhoods. Proc. Natl. Acad. Sci. 116 (14), 6743–6748. https://doi.org/10.1073/pnas.1813145116.

Huang, S.-K., Lindell, M.K., Prater, C.S., 2016. Who leaves and who stays? a review and statistical meta-Analysis of hurricane evacuation studies. Environ. Behav. 48 (8), 991–1029. https://doi.org/10.1177/0013916515578485.

IPCC, 2021. Climate Change 2021: The Physical Science Basis. https://www.ipcc.ch/report/ar6/wg1/.

Jaffe, D.A., O'Neill, S.M., Larkin, N.K., Holder, A.L., Peterson, D.L., Halofsky, J.E., Rappold, A.G., 2020. Wildfire and prescribed burning impacts on air quality in the United States. J. Air Waste Manag. Assoc. 70 (6), 583–615. https://doi.org/10.1080/10962247.2020.1749731.

Jordan, J.R., Cobler, N., 2024. Beryl flooding Houston: Latest weather, location updates. https://www.axios.com/local/houston/2024/07/08/beryl-flooding-houston-tx-weather-now-location-updates.

Karakoc, D.B., Barker, K., Zobel, C.W., Almoghathawi, Y., 2020. Social vulnerability and equity perspectives on interdependent infrastructure network component importance. Sustain. Cities Soc. 57, 102072. https://doi.org/10.1016/j.scs.2020.102072.

Laska, S., Morrow, B.H., 2006. Social vulnerabilities and hurricane katrina: an unnatural disaster in New Orleans. Mar. Technol. Soc. J. 40 (4), 16–26. https://doi.org/10.4031/002533206787353123.

Lee, D.H.K., 1980. Seventy-five years of searching for a heat index. Environ. Res. 22 (2), 331–356. https://doi.org/10.1016/0013-9351(80)90146-2.

Liao, Z., Chen, Y., Li, W., Zhai, P., 2021. Growing threats from unprecedented sequential flood-Hot extremes across China. Geophys. Res. Lett. 48 (18). https://doi.org/10.1029/2021gl094505.

Liu, C., et al., 2025a. Urban flood depth prediction and visualization based on the XGBoost-SHAP model. Water Resources Management, 39 (3), 1353–1375. https://doi.org/10.1007/s11269-024-04020-6.

Lin, N., Emanuel, K., Oppenheimer, M., Vanmarcke, E., 2012. Physically based assessment of hurricane surge threat under climate change. Nat. Clim. Change 2 (6), 462–467. https://doi.org/10.1038/nclimate1389.

Lin, N., Feng, K., Gori, A., Xi, D., Ouyang, M., Oppenheimer, M., 2024. Hurricane Ida's blackout-heatwave compound hazard risk in a changing climate. Res. Sq. https://doi.org/10.21203/rs.3.rs-4096843/v1.
Lindell, M.K., Perry, R.W., 2012. The protective action decision model: theoretical modifications and additional evidence. Risk Anal. 32 (4), 616–632.
Liu, Y., Wang, H., Guan, X., Meng, Y., Xu, H., 2025b. Urban flood depth prediction and visualization based on the XGBoost-SHAP model. Water Resour. Manag. 39 (3), 1353–1375. https://doi.org/10.1007/s11269-024-04020-6.
Long, E.F., Chen, M.K., Rohla, R., 2020. Political storms: emergent partisan skepticism of hurricane risks. Sci. Adv. 6 (37), eabb7906.
Loughnan, M., Nicholls, N., Tapper, N., Mortality–temperature thresholds for ten major population centres in rural Victoria, Australia. 2010. Health Place 16 (6) 1287–1290. https://doi.org/10.1016/j.healthplace.2010.08.008.
Lu, S., Fang, Z., Zhang, X., Shaw, S.-L., Yin, L., Zhao, Z., Yang, X., 2017. Understanding the representativeness of mobile phone location data in characterizing human mobility indicators. ISPRS Int. J. Geo-Inf. 6 (1). https://doi.org/10.3390/ijgi6010007.
Lundberg, S.M., Lee, S.-I., 2017. A unified approach to interpreting model predictions. in: Proceedings of the 31st International Conference on Neural Information Processing Systems, 4768–4777.
Marsooli, R., Lin, N., Emanuel, K., Feng, K., 2019. Climate change exacerbates hurricane flood hazards along US Atlantic and Gulf Coasts in spatially varying patterns. Nat. Commun. 10 (1). https://doi.org/10.1038/s41467-019-11755-z.
Matthews, T., Wilby, R.L., Murphy, C., 2019. An emerging tropical cyclone–deadly heat compound hazard. Nat. Clim. Change 9 (8), 602–606. https://doi.org/10.1038/s41558-019-0525-6.
Mitsova, D., Esnard, A.-M., Sapat, A., Lai, B.S., 2018. Socioeconomic vulnerability and electric power restoration timelines in Florida: the case of Hurricane Irma. Nat. Hazards 94 (2), 689–709. https://doi.org/10.1007/s11069-018-3413-x.
National Centers for Environmental Information, 2024. VIIRS Nighttime Light Data NOAA. https://www.ngdc.noaa.gov/eog/viirs/download_dnb_composites.html.
National Centers for Environmental Information, 2024. National Centers for Environmental Information https://www.ncei.noaa.gov/.
Nicholls, N., Skinner, C., Loughnan, M., Tapper, N., 2008. A simple heat alert system for Melbourne, Australia. Int. J. Biometeorol. 52, 375–384. https://doi.org/10.1007/s00484-007-0132-5.
National Hurricane Center, 2026. Eastern Pacific Tropical Weather Outlook NOAA. https://www.nhc.noaa.gov/refresh.shtml?epac=&utm.
NOAA, 2024. Hurricane Beryl brings massive power outages to East Texas. https://www.nesdis.noaa.gov/news/hurricane-beryl-brings-massive-power-outages-east-texas.
Pace, R.K., LeSage, J.P., 2009. Introduction to Spatial Econometrics. CRC Press
Perkins-Kirkpatrick, S.E., Lewis, S.C., 2020. Increasing trends in regional heatwaves. Nat. Commun. 11 (1). https://doi.org/10.1038/s41467-020-16970-7.
Reinhardt, G.Y., 2015. Race, trust, and return migration. Polit. Res. Q. 68 (2), 350–362. https://doi.org/10.1177/1065912915575790.
Reuters, 2024. CenterPoint misses third-quarter estimates on higher costs, Beryl-related outages. https://www.reuters.com/business/energy/centerpoint-misses-third-quarter-estimates-higher-costs-beryl-related-outages-2024-10-28.
Rodriguez, A.H.A., Shafieezadeh, A., Yilmaz, A., 2022. How important are socioeconomic factors for hurricane performance of power systems?. in: 2022 IEEE International Conference on Power Systems Technology (POWERCON), pp. 1–6.
Rodríguez-Avellaneda, A.H., Rodriguez, R., Shafieezadeh, A., Yilmaz, A., 2025. Socioeconomic disparities in hurricane-induced power outages: insights from multi-hurricane data in florida using XGBoost. Sustain. Cities Soc. 126, 106362. https://doi.org/10.1016/j.scs.2025.106362.
Román, M.O., Stokes, E.C., Shrestha, R., Wang, Z., Schultz, L., Carlo, E., …, Neigh, C.S.R., 2019. Satellite-based assessment of electricity restoration efforts in puerto rico after hurricane maria. PLOS ONE 14 (6), e0218883. https://doi.org/10.1371/journal.pone.0218883.
Román, M.O., Wang, Z., Sun, Q., Kalb, V., Miller, S.D., Molthan, A., …, Masuoka, E.J., 2018. NASA's black marble nighttime lights product suite. Remote Sens. Environ. 210, 113–143. https://doi.org/10.1016/j.rse.2018.03.017.
Sheller, M., 2018. Mobility Justice: The Politics of Movement in an Age of Extremes. Verso Books.
Shi, K., Huang, C., Yu, B., Yin, B., Huang, Y., Wu, J., 2016. Evaluation of NPP-VIIRS night-time light composite data for extracting built-up urban areas. Remote Sens. Lett. 7 (4), 305–314.
Sinclair, M., Maadi, S., Zhao, Q., Hong, J., Ghermandi, A., Bailey, N., 2023. Assessing the socio-demographic representativeness of mobile phone application data. Appl. Geogr. 158, 102997. https://doi.org/10.1016/j.apgeog.2023.102997.
Steadman, R.G., 1984. A universal scale of apparent temperature. J. Clim. Appl. Meteorol. 23 (12), 1674–1687.
Stough, L.M., Sharp, A.N., Resch, J.A., Decker, C., Wilker, N., 2016. Barriers to the long-term recovery of individuals with disabilities following a disaster. Disasters 40 (3), 387–410. https://doi.org/10.1111/disa.12161.
Synolakis, C.E., Karagiannis, G.M., 2024. Wildfire risk management in the era of climate change. PNAS Nexus 3 (5), pp. 151. https://doi.org/10.1093/pnasnexus/pgae151.
Tung Nguyen-Duy, Ngo-Duc, T., Dzung Nguyen-Le, Nguyen-Xuan, T., Tan Phan-Van, 2024. Identification and trend analysis of compound meteorological hazards along Vietnam's coastline. Nat. Hazards 120 (6), 5667–5683. https://doi.org/10.1007/s11069-024-06486-4.
U.S. National Weather Service, 2024. Natural hazard statistics: weather-related fatality and injury statistics https://www.weather.gov/hazstat/.
U.S. Census Bureau, 2022. American community survey 5-year estimates data profiles, 2017–2021. https://data.census.gov.
U.S. Department of Energy, 2021. Protecting our electric grid: Hardening infrastructure against natural disasters.
van Valkengoed, A.M., Steg, L., 2019. Meta-analyses of factors motivating climate change adaptation behaviour. Nat. Clim. Change 9 (2), 158–163. https://doi.org/10.1038/s41558-018-0371-y.
Washington, V., Guikema, S., Mondisa, J.-L., Misra, A., 2024. A data-driven method for identifying the locations of hurricane evacuations from mobile phone location data. Risk Anal. 44 (2), 390–407. https://doi.org/10.1111/risa.14188.
Wu, J., Chen, Y., Liao, Z., Gao, X., Zhai, P., Hu, Y., 2022. Increasing risk from landfalling tropical cyclone-heatwave compound events to coastal and inland china. Environ. Res. Lett. 17 (10), 105007. https://doi.org/10.1088/1748-9326/ac9747.
Xi, D., Lin, N., Gori, A., 2023. Increasing sequential tropical cyclone hazards along the US East and Gulf coasts. Nat. Clim. Change 13 (3), 258–265. https://doi.org/10.1038/s41558-023-01595-7.
Yabe, T., Ukkusuri, S.V., 2020. Effects of income inequality on evacuation, reentry and segregation after disasters. Transp. Res. D Transp. Environ. 82, 102260. https://doi.org/10.1016/j.trd.2020.102260.
Yabe, T., Tsubouchi, K., Fujiwara, N., Sekimoto, Y., Ukkusuri, S.V., 2020. Understanding post-disaster population recovery patterns. J. R. Soc. Interface 17 (163), 20190532. https://doi.org/10.1098/rsif.2019.0532.
Younes, H., Darzi, A., Zhang, L., 2021. How effective are evacuation orders? An analysis of decision making among vulnerable populations in florida during hurricane irma. Travel Behaviour and Society 25, 144–152. https://doi.org/10.1016/j.tbs.2021.07.006.
Zhang, J., Ma, X., Zhang, J., Sun, D., Zhou, X., Mi, C., Wen, H., 2023. Insights into geospatial heterogeneity of landslide susceptibility based on the SHAP-XGBoost model. J. Environ. Manag. 332, 117357. https://doi.org/10.1016/j.jenvman.2023.117357.
Zscheischler, J., Westra, S., van den Hurk, B.J.J.M., Seneviratne, S.I., Ward, P.J., Pitman, A., …, Zhang, X., 2018. Future climate risk from compound events. Nat. Clim. Change 8 (6), 469–477. https://doi.org/10.1038/s41558-018-0156-3.
Zscheischler, J., Martius, O., Westra, S., Bevacqua, E., Raymond, C., Horton, R.M., …, Zscheischler, J., 2020. A typology of compound weather and climate events. Nat. Rev. Earth Environ. 1 (7), 333–347. https://doi.org/10.1038/s43017-020-0060-z.